

A Comprehensive Generalized Theory and Classification of Multiphase Systems for Rotating and Linear Electric Machines

Nicola Campagna, *Member, IEEE*, Massimo Caruso, Antonino Oscar Di Tommaso, Rosario Miceli, *Member, IEEE*

Abstract—The growing interest in electrical machines equipped with multiphase configurations has directed the research to the conception of new design methods and optimization strategies to maximize the performance and the efficiency of the machine for its specific application. In this context, a noticeable gap persists in the comprehensive generalized theory of multiphase systems applied to electrical machines. Therefore, this article aims to propose a new possible classification of multiphase systems based on the electrical symmetries between the corresponding star of slots phasors, starting from the general law related to the spatial distribution of the air-gap magnetic flux density field. This theory extends beyond symmetrical configurations, encompassing both reduced and normal systems, which can be derived from redundant multiphase configurations. Furthermore, the proposed generalization applies to all possible m -phase configurations, including the structures with slight asymmetries or unbalances. The article provides illustrative examples to reinforce these theoretical concepts to establish a systematic and unified theory and classification that can be adopted for any possible topology of a multiphase system.

Index Terms—Electrical machines, multiphase systems, multi-phase winding, winding design.

ϕ_k	phase-shift
b_k^+	progressive wave
b_k^-	regressive wave
Ω_ν	speed of b for each harmonic
ω	electric pulsation
\mathbb{G}	set of integer even numbers
\mathbb{U}	set of integer odd numbers
γ	general symmetrical component
λ	order of the phasor within each symmetrical component
$\alpha = e^{j(2/3)\pi}$	rotating operator

I. INTRODUCTION

ELECTRICAL machines equipped with multiphase configuration have recently gained significant relevance as an interesting alternative to their traditional three-phase counterparts, especially in several applications that demand enhanced overall system reliability and reduced power consumption. This heightened interest can be attributed to their inherent fault-tolerant capabilities, which offer clear advantages in numerous safety-critical working environments such as aerospace and automotive [1], [2]. In addition, multiphase machines deliver increased efficiency and flexibility with lower torque ripple compared to machines designed with conventional three-phase windings. For instance, Cao et al suggest that multiphase machines could become a preferred choice for various aerospace applications [3], whereas Jung et al propose a nine-phase permanent magnet motor for ultrahigh-speed elevators [4], highlighting the advantages of the adoption of multiphase systems.

In recent years, several typologies of multiphase electrical machines have been proposed, from radial to axial-flux structures, from conventional to innovative geometries to provide improved reliability and lower weight, offering high-quality MMF (Magneto Motive Force) with a reduced number of slots per pole per phase [5], [6], [7]. In this area, it can be stated that the design of stator windings significantly influences their overall performance: recent studies have, indeed, introduced innovative strategies for optimizing winding design, encompassing multilayer configurations [8], [9], [10], or developing methodologies devoted to the performance enhancement of these machines, from generalized techniques to suppress specific sets of MMF harmonics [11], [12], to control procedures for independently control multiple air-gap magnetic fields [13]. Undoubted advantages are provided by these techniques, allowing torque density improvement, and decreasing, in the

NOMENCLATURE

Symbol	Quantity
m	number of phases
l	number of layers
p	number of pole pairs
δ	air-gap width
τ	pole pitch
θ	generic angle with respect to vertical axis
N	number of slots
q	number of slots per pole per phase
k	phase section
ν	harmonic order
μ_0	permeability of the vacuum
s	number of non-parallel conductors per slot
$k_{w\nu}$	winding factor of ν -th harmonic
x_0	generic reference angle
x_{0k}	phase-shift between the magnetic axes
B_{xk}	maximum first harmonic magnetic flux density
I_{xk}	amplitude of the k^{th} phase current

Nicola Campagna, Massimo Caruso, Antonino Oscar Di Tommaso and Rosario Miceli are with the Department of Engineering, University of Palermo, Palermo, PA 90128 Italy (e-mail: nicola.campagna@unipa.it, massimo.caruso16@unipa.it, antoninooscarditommaso@unipa.it, rosario.miceli@unipa.it).

meantime, torque ripple, vibrations, acoustic noise, saturation, overall winding losses and harmonic distortion of the back-electromotive force. Therefore, these innovative approaches aim to generate novel and flexible winding designs with the potential to enhance machine efficiency and reduce the amount of copper in stator windings towards a comprehensive solution to the winding design optimization problem, generalizing these approaches to multiphase systems.

Moreover, it can be generally stated that some of the main parameters that characterize the design of an multiphase winding are m , q , and l [14], [15]. Concerning the first parameter, the major trend of the ongoing research has been directed towards the design of multiple three-phase machines, such as the dual three-phase winding configuration [16], [17], [18], consisting of two groups of three-phase windings spatially shifted by 30° between each other. The multi-three-phase configuration has been extensively analyzed in the recent literature, due to the important features brought by this structure, such as enhanced winding factor, lower eddy losses, torque and MMF harmonics [19], [20], [21], [22]. Regarding q , an important recent trend consists of the design of fractional-slot concentrated windings (FSCW), due to their easier and simpler fabrication if compared with distributed layouts [23], [24], [25], [9]; in addition, the shorter end-connections provide lower copper volume, leading to lower weight, higher slot filling factor and, of course, lower copper losses and overall costs and reduced end-winding leakage inductance (though increasing differential leakage inductances) [26]. The high slot fill factor and simplicity of both design and fabrication offered by FSCW topologies make them well-suited for automatic manufacturing in specific industry and automotive applications [27], [28]. However, the MMF harmonic content in FSCW is considerably high due to relevant sub-harmonics, leading to higher torque ripple and rotor losses and consequently reducing the performance of the machine. Thus, many research units have theoretically and experimentally developed generalized algorithms that cover the area of electric machines design with more than three phases that optimize this specific winding configurations [10], [29], [30], [31]. In addition, in certain pole-slots combinations, the harmonic leakage inductance can be considerably higher than the magnetizing inductance, resulting in a lower power factor; to avoid this critical aspect, the harmonic leakage coefficient can be reduced by adequately acting on the winding layers and the phase belt [32].

Finally, regarding the winding design in terms of the number of layers l , many researchers state that winding layouts with $l = 1$ are commonly employed in m -phase machines with prime number of phases (*i.e.*, five-phase, seven-phase and so on), offering high slot filling factor and reduced requirements in terms of insulation [5]. On the other hand, the previously mentioned multiple three-phase machines are often equipped with $l = 2$ layers winding configurations offering higher overall performance [33], whereas windings with $l > 2$ require an accurate selection of the proper slot/pole combination [25].

Despite the undoubted advantages provided by the adoption of multiphase machines, it appears evident that employing a greater number of phases introduces higher complexity during the machine design phase and necessitates more intricate con-

trol methods for the associated electric drive, power converters and their control [34], [35]. Therefore, several challenges lie ahead, including adapting three-phase control structures to multiphase systems and developing accurate fault detection algorithms [36], [37].

Even though the theory regarding three-phase winding configurations in electrical machines has been widely covered in many textbooks and research papers, there is a lack, at present day and from the Author's knowledge, in terms of theory generalized to multiphase machines, leading to some confusion and incompleteness in recent literature. In this context, due to this ever-increasing interest in electrical machines equipped with m -phase systems, this article aims to provide a generalized theory and classification of multiphase redundant, reduced and normal winding configurations, which, at present days, has not been completely reported in detail.

In particular, by taking into account the general law related to the spatial distribution of the magnetic flux density field, this theory covers the description of non-redundant systems, derived from systems in which pairs of phase MMF are placed on the same magnetic axes [38], [39]. These configurations are simplified by deleting the MMF phasors from π to 2π so that the redundancy can be avoided (the contribution in terms of rotating magnetic field would be the same). In the reduced configurations, by shifting a specific group of phasors, the neutral point can be unloaded, avoiding the need of the related conductor. Therefore, as explained in detail in the next sections, every reduced system can be always obtained from a redundant configuration with a doubled number of phases. Some examples are also provided to classify this theory. Moreover, the proposed generalization is also applicable to m -phase windings with slight asymmetries or unbalances, intended as the ratio between the reverse and direct sequences of the winding factor corresponding to that specific winding configuration [40]. These topologies of winding configurations with slight asymmetries can be a valuable option for the electrical machine design since the performance in terms of torque ripple, Maxwell stress tensor, generated torque and current space harmonics are comparable with electrical machines equipped with perfectly symmetrical topologies [26], [41].

Therefore, the main purpose of this work is to provide a systematic and unified theory and classification of electric machines equipped with general multiphase windings, introducing a new possible classification of multiphase systems. More in detail, the paper is structured as follows: Section 2 presents the theory related to the generation of a magnetic field by an m -phase winding; Section 3 reports the classification of multiphase systems based on their features in terms of magnetic redundancy and number of phases; Section 4 describes the theory related to the generation of a magnetic field from unbalanced systems with a particular focus on the point of view of symmetrical components.

II. MAGNETIC FIELD PRODUCED BY AN M-PHASE WINDING

Without affecting the generality of the proposed theory, let's consider a multiphase single-layer (two zones) winding with m phases and, for simplicity, with $p = 1$ pole pair,

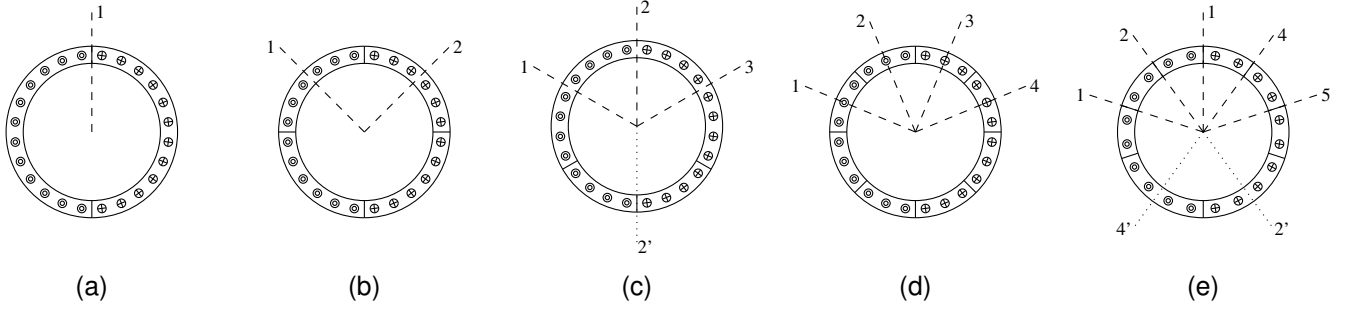


Fig. 1. Two-zones multiphase winding schemes with $p = 1$: (a) single-phase, (b) two-phase, (c) three-phase, (d) four-phase, (e) five-phase.

as shown in Fig. 1. As a further hypothesis, the magnetic axes of the m phases are spatially shifted by a distance τ/m , covering a mechanical angle equal to π/pm [rad]. The spatial configurations from single-phase to five-phase distribution are all reported in Fig. 1 (a-e) [39].

By considering an electrical machine with N slots and q slots per pole and per phase (e.g. $N/2m$ coils for each phase section), neglecting the iron magnetic voltage drops, the general formula of the spatial distribution of the magnetic flux density field generated by the k^{th} phase section at the working harmonic $\nu = 1$ is given by:

$$\begin{aligned} b_{1k}(x, t) &= \\ &= \frac{\mu_0 w k w_1}{\pi p \delta} \cos \left[\frac{\pi}{\tau} (x - x_0 - x_{0k}) \right] \cdot I_{xk} \cos [\omega t - \phi_k] = \\ &= B_{1xk} \cos \left[\frac{\pi}{\tau} \left(x - x_0 - (k-1) \frac{\tau}{m} \right) \right] \cdot \cos [\omega t - \phi_k], \end{aligned} \quad (1)$$

where $w = pqs$, I_{xk} is the amplitude of the current flowing through the k^{th} phase with proper phase-shift ϕ_k , which is supposed to follow the sinusoidal law variability:

$$i_k(t) = I_{xk} \cdot \cos[\omega t - \phi_k]. \quad (2)$$

As graphically shown in Fig. 2, it is well known that a pulsating wave can be represented by the composition of two waves, namely v_1^+ and v_1^- , with equal amplitude (half of the amplitude of the initial wave), propagating in opposite directions. This decomposition can also be analytically discussed by expressing (1) as the sum of two spatial cosine waves:

$$b_{1k}(x, t) = b_{1k}^+(x, t) + b_{1k}^-(x, t), \quad (3)$$

in which the terms $b_{1k}^+(x, t)$ and $b_{1k}^-(x, t)$ are equal to:

$$\begin{aligned} b_{1k}^+(x, t) &= \frac{B_{1xk}}{2} \cos \left[\frac{\pi}{\tau} \left(x - x_0 - (k-1) \frac{\tau}{m} \right) - \omega t + \phi_k \right], \\ b_{1k}^-(x, t) &= \frac{B_{1xk}}{2} \cos \left[\frac{\pi}{\tau} \left(x - x_0 - (k-1) \frac{\tau}{m} \right) + \omega t - \phi_k \right]. \end{aligned} \quad (4)$$

The first one, b_{1k}^+ rotates clockwise and is known as a progressive wave, whereas the second one, b_{1k}^- rotates counterclockwise and is defined as a regressive wave.

By considering (4), the overall effect, due to each of the m phases of the corresponding winding, can be evaluated by summing the contribution of each phase pulsating field. Moreover, by imposing equal peak values of all the m -phase currents, which implies that flux densities $B_{1x1} = B_{1x2} =$

$\dots = B_{1xm} = B_x$, the distribution of the air-gap flux density field is given by (5).

$$\begin{aligned} b(x, t) &= \frac{B_x}{2} \sum_{k=1}^m \cos \left[\frac{\pi}{\tau} \left(x - x_0 - (k-1) \frac{\tau}{m} \right) - \omega t + \phi_k \right] + \\ &+ \frac{B_x}{2} \sum_{k=1}^m \cos \left[\frac{\pi}{\tau} \left(x - x_0 - (k-1) \frac{\tau}{m} \right) + \omega t - \phi_k \right]. \end{aligned} \quad (5)$$

In order to cancel the contribution of the regressive wave (i.e. $\sum_{k=1}^m b_k^- = 0$), the phases of the cosine in the second term of the sum in (5) must be uniformly distributed over 2π . This implies that the phase angle of each k -th current must be equal to:

$$\phi_k = (k-1) \frac{\pi}{m}. \quad (6)$$

Therefore, $b(x, t)$ can be expressed as:

$$\begin{aligned} b(x, t) &= \sum_{k=1}^m [b_k^+(x, t) + b_k^-(x, t)] = \\ &= \frac{B_x}{2} \sum_{k=1}^m \cos \left[\frac{\pi}{\tau} (x - x_0) - \omega t \right] + \\ &+ \frac{B_x}{2} \sum_{k=1}^m \cos \left[\frac{\pi}{\tau} (x - x_0) + \omega t - (k-1) \frac{2\pi}{m} \right]. \end{aligned} \quad (7)$$

By substituting (6) in (5), the first terms of (7) is sum of m cosine waves all having the same phase, whereas the second term is a sum of m cosine functions with mutual phase-shifts equal to $2\pi/m$, which is, thus, null. Therefore, the air-gap magnetic flux density field is equal to:

$$b(x, t) = \frac{mB_x}{2} \cos \left[\frac{\pi}{\tau} (x - x_0) - \omega t \right]. \quad (8)$$

The speed of $b(x, t)$, for each ν^{th} harmonic, is given by:

$$\Omega_\nu = \frac{\omega}{\nu p}. \quad (9)$$

In conclusion, in order to obtain an air-gap rotating magnetic field, the currents supplying the m -phase winding must be temporally shifted by mutual angles of $\phi = \pi/m$, so that the phase of the general k -current can satisfy (6). Moreover, as highlighted in the hypothesis, the magnetic axes of the phases must have a mutual spatial displacement of τ/m , corresponding to an angle of π/pm .

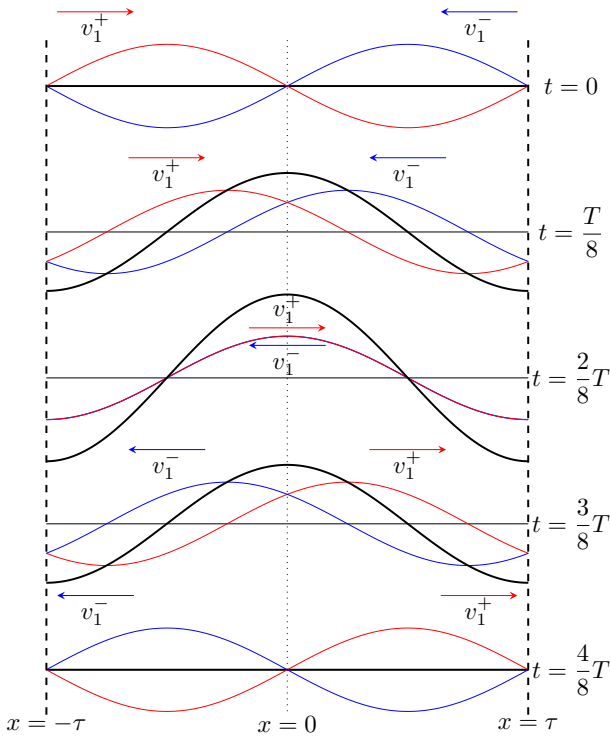


Fig. 2. Representation of the composition of a pulsating wave during different time instants.

III. CLASSIFICATION OF MULTIPHASE SYSTEMS

The theory here presented is valid for any possible m -phase configuration; the authors report here a possible classification of multiphase systems, from single-phase ($m = 1$) to twelve-phase ($m = 12$) configuration, shown in Table I. The systems with a higher number of phases can be treated with the same logic hereinafter reported. In particular, the second column of Table I defines the so-called reduced systems [38], which are characterized by an uniform electrical angular distribution of the m phases in the range $0 \leq \theta < \pi$ (the corresponding magnetic axes of the m phases are spatially shifted by an angle equal to π/pm [rad]). However, such systems present a non-zero homopolar component (the sum of the m phasors is always not zero), which implies the adoption of a neutral conductor (in the case of currents). The third column of Table I reports the normal systems, which are characterized by an odd number of phases with an electrical angular distribution in the range $0 \leq \theta < 2\pi$. Finally, in the last column, the redundant systems are shown. They are characterized also by phasors that are phase-shifted by an angle equal to:

$$\phi'_k = (k - 1) \frac{2\pi}{m}, \quad (10)$$

but, with $m \in \mathbb{G}$.

As it can be noted from Table I, reduced systems with a number of phases equal to m can always be derived from an equivalent redundant system with $m' = 2m$ phases by simply canceling the magnetically redundant phases in the range $\pi \leq \theta < 2\pi$ acting in the same magnetic axes of phases located in the $0 \leq \theta < \pi$ angular region. It can be stated

that both reduced and normal systems can be obtained from redundant configurations, which intrinsically have an even number of phases. It is evident that the same magnetic field produced by a redundant m' -phase system can be produced by an $m'/2$ -phase system because in redundant systems, phasors are displaced two by two in opposite direction, along the same magnetic axis. Redundant systems are here reported as a basic configuration from which it is possible to derive both normal and reduced system. In both normal and redundant systems, the connection of the phases can be realized in either star or polygonal configurations, without any constraint.

The following subsections describe in more detailed some properties of the previously reported systems, in which two main cases can be identified: even and odd number of phases. In particular, the authors show that system with an odd number of phases can be treated in the same way of the most common three-phase systems, whereas systems with an even number of phases have a more complex classification since they can be divided in two main categories: m power of two and m containing an odd prime factor. The latter can be led back to groups of odd-phase systems, while the ones with m power of two have not practical use because they cannot yield pure current systems, as will be shown in the next subsections.

A. Multiphase systems with even number of phases

In the case of an even number of phases ($m \in \mathbb{G}$), two possibilities can be distinguished:

1) m is a power of two.

In such a case, the system cannot be arranged into a pure configuration and, therefore, the neutral conductor is always needed, leading to the necessity of $m + 1$ conductors. Typically, the neutral conductor is loaded more than the phases, even if the homopolar component h_n can be reduced by changing the polarities of the even numbered phases of the multiphase system. Furthermore, these configurations can always be converted to $m/2$ groups of two-phase systems. Indeed, by referring to the configuration with the changed polarities (even numbered phases), to reduce the homopolar current, the system can be arranged into $m/2$ groups of two-phase systems with a phase-shift equal to:

$$\frac{m + 1}{m} \pi, \quad (11)$$

as shown in Table II. In particular, the phasors whose polarity has been changed (even numbered phases) are represented in red color. In the case of $m = 4$ (second column), the two groups are represented by phasors 1-3 and 2-4, phase-shifted by an angle equal to 225° . In the case of $m = 8$, the four groups are represented by the couples 1-5, 2-6, 3-7, 4-8, whose mutual phase-shift is equal to 202.5° . Besides, in this particular configuration, the polygonal connection cannot be provided.

2) m contains an odd prime factor m_u .

In the case of m containing an odd prime factor (e.g., systems with $m = 6 = 2 \cdot 3$ contain $m_u = 3$, whereas for $m = 10$ the odd factor is $m_u = 5$),

TABLE I
CLASSIFICATION OF MULTIPHASE SYSTEMS.

m	Reduced system	Normal system	Redundant system ($m' = 2m$)	m	Reduced system	Normal system	Redundant system ($m' = 2m$)
1				7			
2		-----		8		-----	
3				9			
4		-----		10		-----	
5				11			
6		-----		12		-----	

the system can be arranged into $m_g = m/m_u$ groups of subsystems with m_u phases, in which the mutual phase-shift is equal to π/m . For instance, a six-phase configuration contains $m_g = 2$ groups of $m_u = 3$ phases with a mutual phase-shift of $\pi/6$, as shown in the first column of Table III, which summarize the examples of these systems. It can be noted that for $m = 10$, $m_g = 2$ groups of $m_u = 5$ phase systems (phase-shift equal to 18°) are identified, whereas the twelve-phase system arranged a $m_g = 4$ groups of $m_u = 3$ phase systems phase-shifted by an angle equal to 15° . It has

to be noted that this kind of systems can be arranged with other possible configurations with respect to the one just presented, but they would be inconvenient, as asymmetrical distributions could occur (*i.e.*, $m/2$ groups of two-phase systems, with the derived phase-shift between the groups, leading to the need a further neutral conductor). Thus, as a systematic rule, such a system can always be decomposed in m_g groups of normal systems, which are well-known, simple and easy to implement both in design of electrical machines and control of electrical drives.

TABLE II
MULTIPHASE SYSTEMS WHERE m IS A POWER OF TWO.

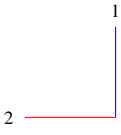
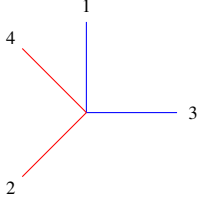
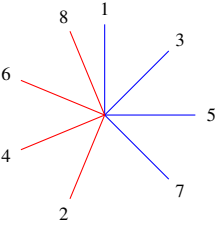
$m = 2$	$m = 4$	$m = 8$
		

TABLE III
MULTIPHASE SYSTEMS WHERE m IS AN EVEN NUMBER CONTAINING AN ODD PRIME FACTOR.

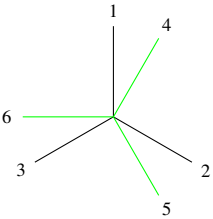
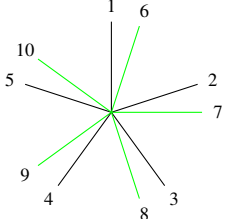
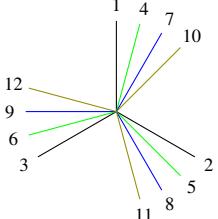

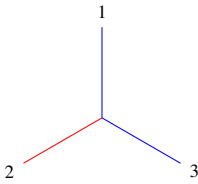
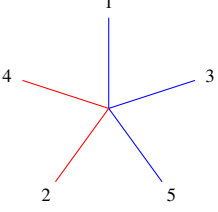
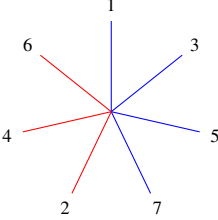
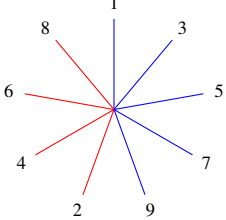
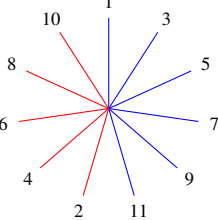
$m = 6$	$m = 10$	$m = 12$
		

TABLE IV
MULTIPHASE SYSTEMS WHERE m IS AN ODD NUMBER.

$m = 1$	$m = 3$	$m = 5$
		
		

B. Multiphase systems with odd number of phases

Dealing with an odd number of phases ($m \in \mathbb{U}$), the reduced system can be always converted to a pure system by changing the polarities of the even numbered phases (e.g. inverting the currents circulating in the even numbered phases), as shown in Table IV (red phasors). In this case, the system can be defined as "pure-reduced", which, by renumbering the phase sequence, defines normal systems, as previously shown in third column of Table I. In any case, for the obtainment of the rotating magnetic field, it is needed that the change of the polarity must be realized also in the corresponding phase section, so that the direction of the produced field is not changed.

IV. AIR-GAP MAGNETIC FIELD PRODUCED BY UNBALANCED SYSTEMS OF M-PHASE CURRENTS

This Section analyses the generation of an air-gap magnetic field in case an unbalanced system of currents supplies an m -phases winding. It is, therefore, needed to examine the decomposition of an unbalanced multiphase system into symmetrical components. The theory hereinafter reported allows to trace back all the possible multiphase systems as affordable configurations. Indeed, independently from the number of phases (even or odd), every system can be treated by applying the generalized Fortescue's theorem. From the classification reported in Section III, the outcomes and advantages of their decomposition in symmetrical components, as well as the

properties of the magnetic field generated by symmetrical components, are distinguished below. Three cases can be identified: redundant systems, normal systems and reduced systems. In particular, it is needed, for the last category, to highlight the differences between even and odd number of phases.

A. Symmetrical Components

From Fortescue's theorem [15], the symmetrical components of a multiphase system composed of n phasors I_1, I_2, \dots, I_n with both random amplitude and angles can be computed as follows:

$$I_\lambda^{(\gamma)} = \frac{\alpha^{\gamma(\nu-1)}}{m} \sum_{n=1}^m \alpha^{\gamma(n-1)} I_n, \quad (12)$$

where $\gamma = 0, 1, \dots, m-1$ is the general symmetrical component at the sequence $0, 1, \dots, m-2$ and $\lambda = 1, 2, \dots, m$ is the order of the phasor within each symmetrical component and α is given by:

$$\alpha = e^{j\frac{2\pi}{m}}. \quad (13)$$

From (12), it is evident that in m -phase systems, the sequence $\gamma = 0$ is always a zero sequence. With reference to the classification proposed in this work, three cases can be considered. In particular, redundant systems (case 1), even though can be treated with the theory of symmetrical components, are not practically used due to their redundancies between phase sections acting along the same magnetic axes. On the contrary, normal systems (case 2) and reduced systems with an odd number of phases (case 3.a) or even number of phases containing an odd prime factor (case 3.b) can be traced back to the generalized theorem, simplifying their treatment with respect to the theory exposed in [14]. Finally, reduced systems with m power of two (case 3.c) are not practically used, due to the need of a neutral conductor.

1) Redundant systems.

In this case, the sequence of order $m/2$ presents $m/2$ pair of phasors in phase opposition between each other. The sequence $\gamma = m/2$ (equal to 3 in the case of a six-phase system, see Fig. 3), is defined as pseudo-zero sequence (Fig. 3 (d)) due to the similar features with sequence zero (Fig. 3 (a)). Moreover, the sequences with order $1 \leq \gamma < \frac{m}{2}$ are defined as direct, whereas sequences with order $\frac{m}{2} > \gamma \leq m-1$ are defined as inverse. For instance, the direct and inverse sequences for a redundant six-phase system are represented in Figs. 3 (b-c) and 3 (e-f), respectively.

2) Normal systems.

In such a case (see Fig. 4), the system can always be decomposed in a zero sequence, $\frac{m-1}{2}$ direct sequences, $\frac{m-1}{2}$ inverse sequences. For instance, a five-phase configuration will be composed of one zero-sequence, two direct sequences (1 and 2) and two inverse sequences (3 and 4), as depicted in Fig. 4 (a-e). The simple case of a three-phase system is composed of one zero sequence, one direct sequence and one inverse sequence.

3) Reduced systems.

a) $m \in \mathbb{U}$.

Reduced systems with an odd number of phases can be included in case no.2 (normal systems), since they can be always converted to a pure system by changing the polarities of the even numbered phases and renumbering the phase sequence, as fully described in Section III.

b) $m \in \mathbb{G}$ containing an odd prime factor.

Reduced systems with an even number of phases, with m containing an m_u prime factor (*i.e.* $m = 6, 10, 12, \dots$), can be arranged into m_g groups of m_u -phase systems. It means that the system can be decomposed in m_g zero sequences, $m_g \binom{m_u-1}{2}$ direct sequences and $m_g \binom{m_u-1}{2}$ inverse sequences. Fig. 5 shows the decomposition of a six-phase reduced system. In particular, Fig. 5(a) is referred to the $m_g = 2$ zero sequences ($\gamma = 0, 3$), whereas Fig. 5(b) and (c) report the $m_g \binom{m_u-1}{2} = 2$ direct sequences ($\gamma = 1, 4$) and inverse sequences ($\gamma = 2, 5$), respectively.

c) $m \in \mathbb{G} \mid m = 2^n$.

In this case, according to (12) it has to be noted that zero and pseudo-zero sequences will not appear since this type of systems can always be decomposed into $m/2$ two-phase systems (each of one has not zero sequence). When considering these systems, only direct and inverse sequences can be detected. Fig. 6 shows, as an example, the direct and inverse sequence of the reduced four-phase system. In particular, 6 (a) is representative of the $m/2 = 2$ direct sequences, whereas 6 (b) plots the $m/2 = 2$ inverse sequences.

B. Rotating magnetic fields generated by symmetrical components

This Section analyses the contribution of each symmetrical component to the generation of a rotating magnetic field. For this purpose, by considering an m -phase redundant, normal or reduced system with $m \in \mathbb{U}$ (with changed polarities of the even numbered phases) with magnetic axes spatially shifted by an angle equal to $2\pi/m$, the pulsating flux density field generated by the symmetrical component at the γ^{th} sequence that supplies the k^{th} phase is given by:

$$\begin{aligned} b_{1k}^{(\gamma)}(x, t) &= B_{1xk}^{(\gamma)} \cos \left[\frac{\pi}{\tau} \left(x - x_0 - (k-1) \frac{2\tau}{m} \right) \right] \cos(\omega t - \phi_{k\gamma}) = \\ &= \frac{B_{1xk}^{(\gamma)}}{2} \cos \left[\frac{\pi}{\tau} (x - x_0) - (k-1) \frac{2\pi}{m} - \omega t + \phi_k \right] + \\ &+ \frac{B_{1xk}^{(\gamma)}}{2} \cos \left[\frac{\pi}{\tau} (x - x_0) - (k-1) \frac{2\pi}{m} + \omega t - \phi_k \right]. \end{aligned} \quad (14)$$

where

$$B_{xk}^{(\gamma)} = \frac{\mu_0 \omega k_{w1}}{\pi p \delta} I_{xk}^{(\gamma)} = \sqrt{2} \frac{\mu_0 \omega k_{w1}}{\pi p \delta} I_k^{(\gamma)} \quad (15)$$

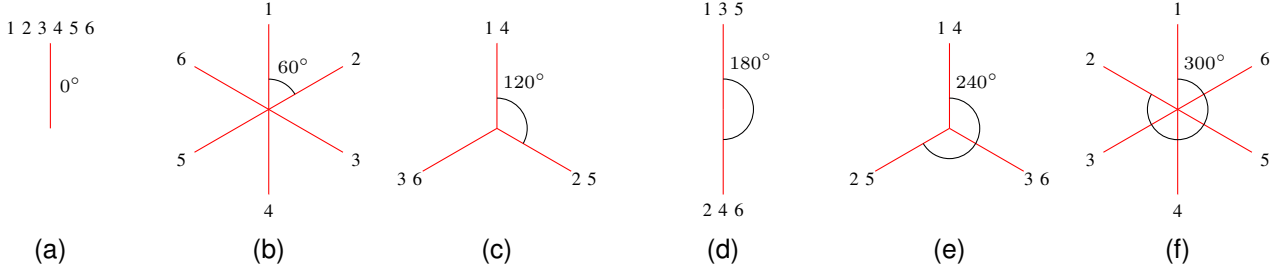


Fig. 3. Symmetrical components of a six-phase redundant (non-reduced) system: (a) homopolar, (b-c) direct, (d) pseudo-homopolar, (e-f) inverse.

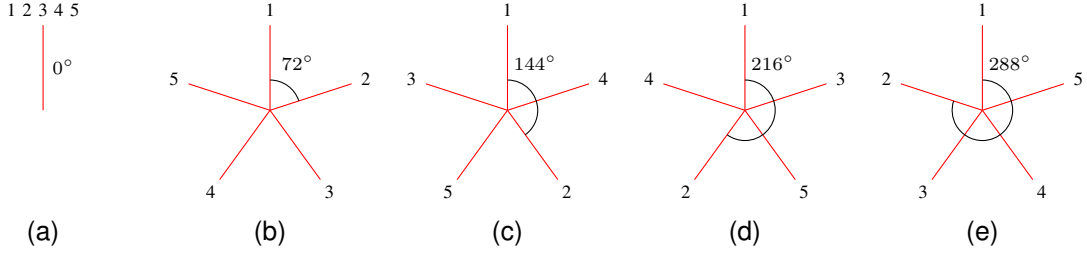


Fig. 4. Symmetrical components of a five-phase normal system: (a) homopolar, (b-c) direct, (d-e) inverse.

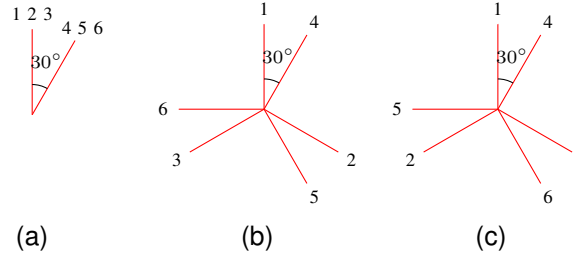


Fig. 5. Symmetrical components of a six-phase reduced system: (a) homopolar, (b) direct, (c) inverse.

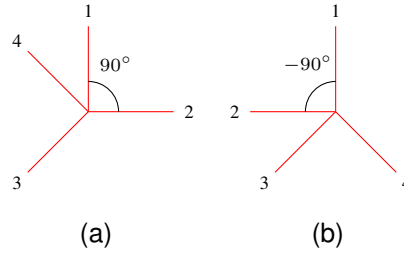


Fig. 6. Symmetrical components of a four-phase reduced system: (a) direct, (b) inverse.

and

$$\begin{aligned} i_k^{(\gamma)}(t) &= I_{xk}^{(\gamma)} \cos \left[\omega t - \gamma(k-1) \frac{2\pi}{m} - \phi \right] = \\ &= \sqrt{2} I_k^{(\gamma)} \cos \left[\omega t - \gamma(k-1) \frac{2\pi}{m} - \phi \right]. \end{aligned} \quad (16)$$

B_{xk} is the maximum value of the flux density field and $i_k^{(\gamma)}(t)$ is the γ^{th} component of the k^{th} current with phase-shift equal to $\phi_{k\gamma}$ which is given by:

$$\phi_{k\gamma} = \gamma(k-1) \frac{2\pi}{m} - \phi \quad (17)$$

in which ϕ is the generic phase angle of the current.

By setting $x_0 = 0$ for simplicity and by considering the contribution of all m phases, for both normal and reduced systems, formula (18) can be obtained.

$$\begin{aligned} b^{(\gamma)}(x, t) &= \sum_{k=1}^m \left[b_k^{(\gamma)+}(x, t) + b_k^{(\gamma)-}(x, t) \right] = \\ &= \frac{B_x^{(\gamma)}}{2} \sum_{k=1}^m \cos \left[\frac{\pi}{\tau} x - (1-\gamma)(k-1) \frac{2\pi}{m} - \omega t + \phi \right] + \\ &+ \frac{B_x^{(\gamma)}}{2} \sum_{k=1}^m \cos \left[\frac{\pi}{\tau} x - (1+\gamma)(k-1) \frac{2\pi}{m} + \omega t - \phi \right]. \end{aligned} \quad (18)$$

$$b^{(\gamma)}(x, t) = \sum_{i=1}^2 \sum_{k=1}^{m/4} \sum_{l=1}^2 \left[b_k^{(\gamma)+}(x, t) + b_k^{(\gamma)-}(x, t) \right] =$$

$$= \frac{B_x^{(\gamma)}}{2} \sum_{i=1}^2 \sum_{k=1}^{m/4} \sum_{l=1}^2 \left\{ \cos \left[\frac{\pi}{\tau} x - (i - \gamma)(l - 1) \frac{\pi}{2} - \omega t + \phi \right] + \cos \left[\frac{\pi}{\tau} x - (i - 1) \frac{m-1}{m} 2\pi - (k-1) \frac{4\pi}{m} - (1 + \gamma)(l - 1) \frac{\pi}{2} + \omega t - \phi \right] \right\}$$

From this equation, it appears clear that the sum is not null only for $\gamma = 1$ and $\gamma = m - 1$, for which $b^{(\gamma)}(x, t)$ is equal, respectively to:

$$b^{(1)}(x, t) = \frac{mB_x^{(1)}}{2} \cos \left(\frac{\pi}{\tau} x - \omega t + \phi \right)$$

$$b^{(m-1)}(x, t) = \frac{mB_x^{(m-1)}}{2} \cos \left(\frac{\pi}{\tau} x + \omega t - \phi \right)$$

while it is equal to 0 for $\gamma = 0$ and $1 \leq \gamma \leq m - 1$.

In the case of reduced systems with $m \neq 2^n$, the expression of the current on the r -th phase, at the γ -th sequence of the i -th group, is given by:

$$i_r^{(\gamma)}(t) = I_{xr}^{(\gamma)} \cos \left[\omega t - (i - 1) \frac{\pi}{m} - \gamma_i(k - 1) \frac{2\pi}{m_u} - \phi \right] =$$

$$= \sqrt{2} I_r^{(\gamma)} \cos \left[\omega t - (i - 1) \frac{\pi}{m} - \gamma_i(k - 1) \frac{2\pi}{m_u} - \phi \right],$$

with

$$\begin{cases} r = m_u(i - 1) + k; \\ k = 1, \dots, m_u; \\ i = 1, \dots, m_g. \end{cases}$$

In order to simplify the discussion, it is assumed that all m_g groups are supplied by the same symmetrical component (i.e., $\gamma_1 = \gamma_2 = \dots = \gamma_{m_g} = \gamma$).

For this case, the expression of the flux density field at the γ -th sequence is given by (22).

$$b^{(\gamma)}(x, t) = \sum_{i=1}^{m_g} \sum_{k=1}^{m_u} \left[b_k^{(\gamma)+}(x, t) + b_k^{(\gamma)-}(x, t) \right] =$$

$$= \frac{B_x^{(\gamma)}}{2} \sum_{i=1}^{m_g} \sum_{k=1}^{m_u} \cos \left[\frac{\pi}{\tau} x - (1 - \gamma)(k - 1) \frac{2\pi}{m_u} - \omega t + \phi \right] +$$

$$+ \frac{B_x^{(\gamma)}}{2} \sum_{i=1}^{m_g} \sum_{k=1}^{m_u} \cos \left[\frac{\pi}{\tau} x - (1 + \gamma)(k - 1) \frac{2\pi}{m_u} - (i - 1) \frac{2\pi}{m} + \omega t - \phi \right].$$

The latest equation is not null only for $\gamma = 1$ and $\gamma = m_u - 1$, $b^{(\gamma)}(x, t)$ it is equal, respectively to:

$$b^{(1)}(x, t) = \frac{mB_x^{(1)}}{2} \cos \left(\frac{\pi}{\tau} x - \omega t + \phi \right)$$

$$b^{(m_u-1)}(x, t) = \frac{m_u B_x^{(m_u-1)}}{2} \frac{\sin \left(\frac{\pi}{m_u} \right)}{\sin \left(\frac{\pi}{m} \right)} \cos \left(\frac{\pi}{\tau} x + \omega t - \phi \right)$$

while it is equal to 0 for $\gamma = 0$ and $1 \leq \gamma \leq m_u - 1$.

Finally, for completeness, in the case of reduced systems with m power of two ($m = 2^n$), although not particularly used in practical applications, the equation is reformulated as:

$$i_r^{(\gamma)}(t) = I_{xr}^{(\gamma)} \cos \left[\omega t - (i - 1) \frac{m+1}{m} \pi - (k - 1) \frac{2\pi}{m} - \gamma(l - 1) \frac{\pi}{2} - \phi \right] =$$

$$= \sqrt{2} I_r^{(\gamma)} \cos \left[\omega t - (i - 1) \frac{m+1}{m} \pi - (k - 1) \frac{2\pi}{m} - \gamma(l - 1) \frac{\pi}{2} - \phi \right].$$

with

$$\begin{cases} r = \frac{m}{4}(i - 1) + 2(k - 1) + l; \\ i = 1, 2; \\ k = 1, \dots, \frac{m}{4}. \end{cases}$$

It has to be noted that in the latest case, for each two-phase group, only the direct and inverse sequences are involved, assuming the values equal to $\gamma = 1$ and $\gamma = m_u - 1$ respectively. In this case of study, the flux density field at the γ^{th} sequence is expressed as in (26).

In general, for reduced systems and depending on the values of γ , $b^{(\gamma)}(x, t)$ is equal to:

$$b^{(\gamma)}(x, t) = \begin{cases} \frac{m}{2} B_x^{(\gamma)} \cos \left(\frac{\pi}{\tau} x - \omega t + \phi \right) \\ \frac{m_u}{2} \frac{\sin \left(\frac{\pi}{m_u} \right)}{\sin \left(\frac{\pi}{m} \right)} B_x^{(\gamma)} \cos \left(\frac{\pi}{\tau} x - \omega t - \phi \right) \end{cases}$$

for $\gamma = 1$ and $\gamma = m_u - 1$, respectively.

In conclusion, the reverse field at the sequence $\gamma = m_u - 1$ produces an air-gap magnetic field that propagates in the reverse direction, and presents a reduced amplitude in comparison to the direct-sequence field equal to:

$$k_{inv} = \frac{m_u \cdot \sin \left(\frac{\pi}{m_u} \right)}{2 \cdot \sin \left(\frac{\pi}{m} \right)} \leq \frac{m}{2}.$$

By analyzing (23) and (27), it appears clear that it is not suitable to reverse the driving sequence for reversing the direction of rotation of the magnetic field, since the obtained rotating field would be, indeed, decreased in magnitude. As an example, for $m = 6$, in the case of two direct symmetrical components, the amplitude of the rotating flux density field is 6 times the value of the flux density produced by each phase; otherwise, in the case of two inverse symmetrical components, the resultant field will rotate in the opposite direction, but with an amplitude equal to:

$$\frac{3 \cdot \sin \left(\frac{\pi}{3} \right)}{\sin \left(\frac{\pi}{6} \right)} = 3\sqrt{3},$$

which means 86.6% of the maximum amplitude.

From the physical point of view, this result derives from the fact that, in the case of two inverse sequences, represented by phasors 1-3-2 and 4-6-5 shown in Fig. 5(c), the field produced by the second three-phase group (phasors 4-6-5) is lagging in space by 60° with respect to the magnetic axis of phase 1, taken as reference. This overall shift is due to the 30° spatial lag of its magnetic axis with respect to the reference and the 30° time lag of the second three-phase current group with respect to magnetic axis of phase 4. Fig. 7(a) shows the

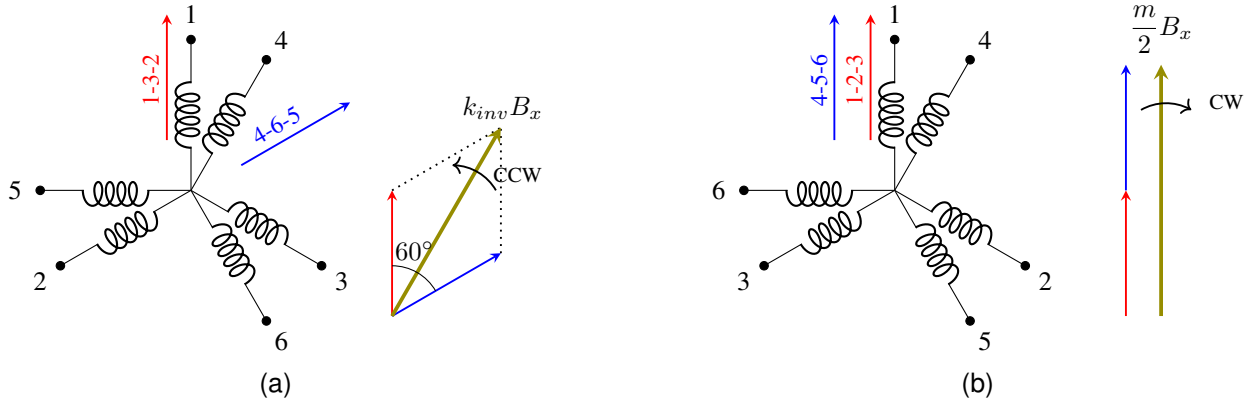


Fig. 7. Spatial disposition of a six-phase winding fed by (a) two inverse sequences, (b) two direct sequences: field produced by the phasors groups and resulting air-gap field.

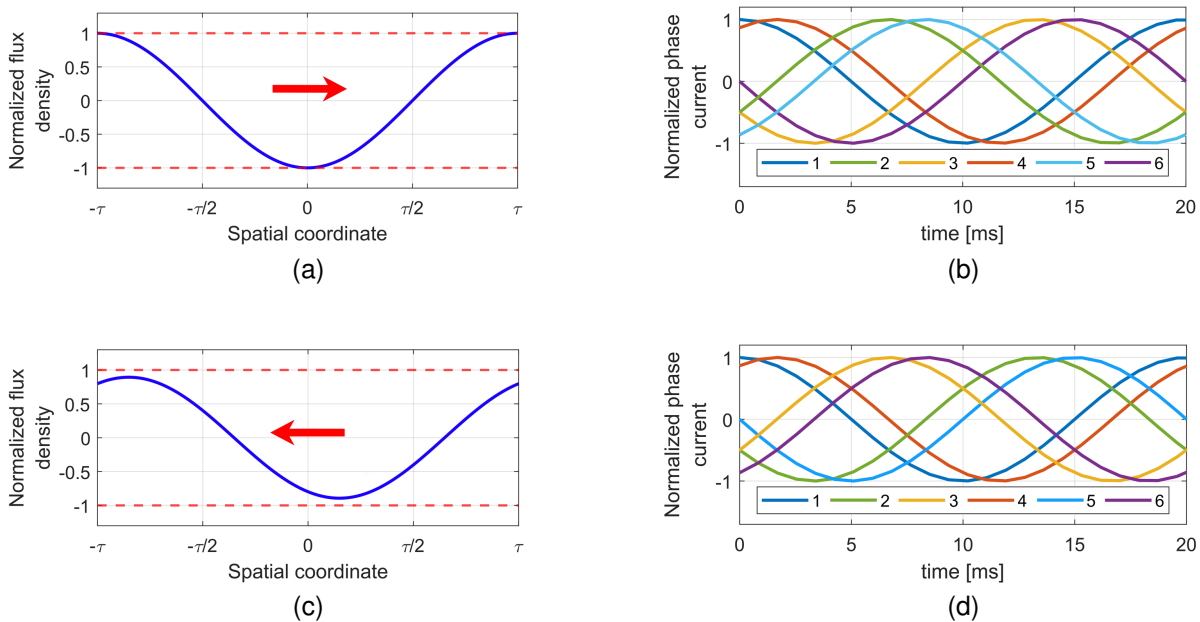


Fig. 8. Magnetic field produced by a six-phase reduced winding fed by (a) two direct sequences, (c) two inverse sequences; six-phase current systems: (b) direct sequences, (d) inverse sequences.

winding spatial disposition and the field generated by the two phasor groups at the time instant in which current in phase 1 has its maximum amplitude. In particular, the red phasor is representative of the field produced by the group 1-3-2, whereas the blue one represents the field generated by the group 4-6-5. In the same subfigure, the resulting air-gap field, with amplitude equal to $k_{inv} \cdot B_x$ and rotating counterclockwise (CCW), is represented in green. It can be noted that the resulting field is equal to the vectorial sum of the fields produced by the two three-phase groups. On the contrary, by feeding the system with two direct sequences, represented by phasors 1-2-3 and 4-5-6 shown in Fig. 5(b), the magnetic field produced by the second three-phase group (phasors 4-5-6) leads by 30° with respect to the magnetic axis of phase 4, so that the resultant field will be aligned with the magnetic axis of phase 1 and the two fields can be added algebraically, as depicted in 7(b). The field generated by the groups 1-2-3 and 4-5-6 are represented in red and blue, respectively. The resulting field, with an

amplitude equal to $\frac{m}{2} \cdot B_x$ and rotating clockwise (CW), is represented in green. A proper solution for the obtainment of the maximum flux density field amplitude, if the system is supplied by inverse sequences, consists of changing the sign of the supply frequency, which can be easily obtained through the adoption of a power converter. The same phenomenon can be discussed from another perspective: indeed, Figs. 8 (a) and (c) show the magnetic field produced by a six-phase, one pole pair and single-layer reduced winding fed by two direct sequences and two inverse sequences, respectively. It can be noted again that the amplitude of the field derived from the two inverse sequences is lower than the one produced by the two direct sequences, according to (28). The arrows represent the traveling direction of the waves in the two considered cases. Figs. 8 (b) and (d) show the six-phase current system feeding the machine in both cases of two direct sequences and two inverse sequences.

V. CONCLUSIONS

The increasing interest in multiphase winding configurations for electrical machines has spurred the development of new design methods and optimization strategies aimed at maximizing performance for specific applications. Notwithstanding the undeniable advantages offered by multiphase machines, the number of possible configurations introduces a significant degree of complexity, particularly for the design phase, leading to the need of defining a theory that generalizes properly the features of multiphase systems. Therefore, this article has presented a comprehensive classification of multiphase systems, including reduced and normal systems derived from the redundant configurations. Different multiphase configurations offer distinct advantages: the proposed classification allows to schematize and simplify the treatment of complex systems, providing a unique methodology for the study of multiphase systems based on their intrinsic properties. This aspect can help to identify easily which configuration is best suited for a specific application. Indeed, through the proposed methodology, each configuration, independently from the number of phases, can be treated and traced back to affordable, well-known systems, easy to study, design and implement. Furthermore, the proposed classification has been integrated with the analysis of the symmetrical components, providing, in general, a deeper understanding of multiphase systems. In particular, in this work, the outcomes and advantages of integrating the proposed classification with the theory of symmetrical components are described, further discussing how each system can be treated by applying the generalized Fortescue theorem and specifying the peculiarities of each configuration, simplifying the treatment of multiphase unbalanced systems.

Key findings of the article are the contribution of a comprehensive framework for understanding and classifying multiphase systems in electrical machines, offering valuable insights for researchers, engineers, and designers. The proposed theory and classification pave the way for further advancements in multiphase electrical machines, addressing both theoretical gaps and practical challenges.

ACKNOWLEDGEMENTS

This research has been partially supported by the European Union - NextGenerationEU - National Sustainable Mobility Center CN00000023, Italian Ministry of University and Research Decree n. 1033—17/06/2022, Spoke 3, CUP B73C22000760001, by the project 'SiciliAn MicronanOTeCH Research And Innovation Center' 'SAMOTHRACE' (MUR, PNRR-M4C2, ECS-00000022),spoke 3 - Università degli Studi di Palermo 'S2-COMMS' - Micro and Nanotechnologies for Smart & Sustainable Communities", by the project "Network 4 Energy Sustainable Transition - NEST", CUP B73C22001280006, Project code PE0000021, Concession Decree No. 1561 of 11.10.202, by the OPTEBUS project (Development of an Optimal Design Tool for Electrification of Urban Public Transportation BUS Services) - PRIN Progetti di Rilevante Interesse Nazionale 2022- PRJ-0969 - ID 42740, by the ESPFET project (Enhanced Energy-Saving Powertrains for Freight E-Transportation) - PRIN Progetti di Rilevante Interesse Nazionale 2022- PRJ-0962- ID 42679.

REFERENCES

- [1] F. Barrero and M. J. Duran, "Recent advances in the design, modeling, and control of multiphase machines 2014;part i," *IEEE Transactions on Industrial Electronics*, vol. 63, no. 1, pp. 449–458, Jan 2016.
- [2] M. J. Duran and F. Barrero, "Recent advances in the design, modeling, and control of multiphase machines 2014;part ii," *IEEE Transactions on Industrial Electronics*, vol. 63, no. 1, pp. 459–468, Jan 2016.
- [3] W. Cao, B. C. Mecrow, G. J. Atkinson, J. W. Bennett, and D. J. Atkinson, "Overview of electric motor technologies used for more electric aircraft (mea)," *IEEE Transactions on Industrial Electronics*, vol. 59, no. 9, pp. 3523–3531, 2012.
- [4] E. Jung, H. Yoo, S.-K. Sul, H.-S. Choi, and Y.-Y. Choi, "A nine-phase permanent-magnet motor drive system for an ultrahigh-speed elevator," *IEEE Transactions on Industry Applications*, vol. 48, no. 3, pp. 987–995, 2012.
- [5] M. Y. Metwly, A. S. Abdel-Khalik, M. S. Hamad, S. Ahmed, and N. A. Elmalhy, "Multiphase stator winding: New perspectives, advanced topologies, and futuristic applications," *IEEE Access*, vol. 10, pp. 103 241–103 263, 2022.
- [6] E. Levi, "Multiphase electric machines for variable-speed applications," *IEEE Transactions on Industrial Electronics*, vol. 55, no. 5, pp. 1893–1909, May 2008.
- [7] E. Levi, R. Bojoi, F. Profumo, H. Toliyat, and S. Williamson, "Multiphase induction motor drives - a technology status review," *Electric Power Applications, IET*, vol. 1, pp. 489 – 516, 08 2007.
- [8] S. Jordan, C. D. Manolopoulos, and J. M. Apsley, "Winding configurations for five-phase synchronous generators with diode rectifiers," *IEEE Transactions on Industrial Electronics*, vol. 63, no. 1, pp. 517–525, Jan 2016.
- [9] A. Tassarolo, C. Ciriani, M. Bortolozzi, M. Mezzarobba, and N. Barbini, "Investigation into multi-layer fractional-slot concentrated windings with unconventional slot-pole combinations," *IEEE Transactions on Energy Conversion*, vol. 34, no. 4, pp. 1985–1996, 2019.
- [10] J. Germishuizen and A. Kremser, "Algebraic design of symmetrical windings for ac machines," *IEEE Transactions on Industry Applications*, vol. 57, no. 3, pp. 1928–1934, 2021.
- [11] A. M. Silva, C. H. Antunes, A. M. S. Mendes, and F. J. T. E. Ferreira, "On phase shifting and diversified coil-pitch for enhanced multiobjective winding design optimization," *IEEE Transactions on Energy Conversion*, vol. 36, no. 3, pp. 2002–2011, 2021.
- [12] W. Yujun, Y. Dejun, and Z. Yan, "Magnetomotive force decomposition and harmonic analysis of fractional-slot concentrated winding," in *2023 8th Asia Conference on Power and Electrical Engineering (ACPEE)*, 2023, pp. 2212–2216.
- [13] F. Nishanth, A. Khamitov, and E. L. Severson, "Design of electric machine windings to independently control multiple airgap harmonics," *IEEE Transactions on Industry Applications*, pp. 1–12, 2023.
- [14] A. A. Rockhill and T. A. Lipo, "A generalized transformation methodology for polyphase electric machines and networks," in *2015 IEEE International Electric Machines and Drives Conference (IEMDC)*, 2015, pp. 27–34.
- [15] C. L. Fortescue, "Method of symmetrical co-ordinates applied to the solution of polyphase networks," *Proceedings of the American Institute of Electrical Engineers*, vol. 37, no. 6, pp. 629–716, June 1918.
- [16] E. L. Soares, C. B. Jacobina, N. B. de Freitas, N. Rocha, A. C. N. Maia, and A. M. N. Lima, "A multilevel open-end winding six-phase induction motor drive topology based on three two-level three-phase inverters," *IEEE Transactions on Industry Applications*, vol. 59, no. 5, pp. 6360–6372, 2023.
- [17] M. K. Pinjala and R. Bhimasingu, "Improving the dc-link utilization of nine-switch boost inverter suitable for six-phase induction motor," *IEEE Transactions on Transportation Electrification*, vol. 6, no. 3, pp. 1177–1187, 2020.
- [18] H. S. Che, M. J. Duran, E. Levi, M. Jones, W.-P. Hew, and N. A. Rahim, "Postfault operation of an asymmetrical six-phase induction machine with single and two isolated neutral points," *IEEE Transactions on Power Electronics*, vol. 29, no. 10, pp. 5406–5416, 2014.
- [19] S. Wang, Z. Zhu, P. Adam, S. Juntao, D. Rajesh, and U. Chiaki, "Comparison of differentwinding configurations for dual three-phase interior pm machines in electric vehicles," *MDPI Energies*, vol. 13, no. 3, 2022.
- [20] Y. Demir and M. Aydin, "A novel dual three-phase permanent magnet synchronous motor with asymmetric stator winding," *IEEE Transactions on Magnetics*, vol. PP, no. 99, pp. 1–1, 2016.

- [21] T. Bringezu and J. Biela, "Comparison of optimized motor-inverter systems using a stacked polyphase bridge converter combined with a 3-, 6-, 9-, or 12-phase pmsm," in *2020 22nd European Conference on Power Electronics and Applications (EPE'20 ECCE Europe)*, 2020, pp. P.1–P.11.
- [22] J. Xing, T. Wang, and D. Wang, "Design and research of modular multiphase permanent magnet direct drive generator," in *2019 22nd International Conference on Electrical Machines and Systems (ICEMS)*, 2019, pp. 1–4.
- [23] A. M. Silva, F. J. T. E. Ferreira, M. V. Cistelean, and C. H. Antunes, "Multiobjective design optimization of generalized multilayer multiphase ac winding," *IEEE Transactions on Energy Conversion*, vol. 34, no. 4, pp. 2158–2167, 2019.
- [24] A. M. EL-Refaie, "Fractional-slot concentrated-windings synchronous permanent magnet machines: Opportunities and challenges," *IEEE Transactions on Industrial Electronics*, vol. 57, no. 1, pp. 107–121, 2010.
- [25] L. Alberti and N. Bianchi, "Theory and design of fractional-slot multilayer windings," *IEEE Transactions on Industry Applications*, vol. 49, no. 2, pp. 841–849, 2013.
- [26] M. Caruso, A. O. D. Tommaso, F. Genduso, R. Miceli, and G. R. Galluzzo, "A general mathematical formulation for the determination of differential leakage factors in electrical machines with symmetrical and asymmetrical full or dead-coil multiphase windings," *IEEE Transactions on Industry Applications*, vol. 54, no. 6, pp. 5930–5940, 2018.
- [27] G. Choi and T. M. Jahns, "Reduction of eddy-current losses in fractional-slot concentrated-winding synchronous pm machines," *IEEE Transactions on Magnetics*, vol. 52, no. 7, pp. 1–4, 2016.
- [28] D.-K. Hong, W. Hwang, J.-Y. Lee, and B.-C. Woo, "Design, analysis, and experimental validation of a permanent magnet synchronous motor for articulated robot applications," *IEEE Transactions on Magnetics*, vol. 54, no. 3, pp. 1–4, 2018.
- [29] Z.-Z. Wu and J.-X. Shen, "Generalized analysis of armature windings mmf harmonics," in *2021 IEEE 4th Student Conference on Electric Machines and Systems (SCEMS)*, 2021, pp. 1–6.
- [30] J. Wu, Q. Xu, and L. Xu, "A study on winding mmf harmonic and vibration of polyphase motor," in *2021 Power System and Green Energy Conference (PSGEC)*, 2021, pp. 732–737.
- [31] D. Lekic and S. Vukosavic, "Optimization of multiphase single-layer winding end-connections by differential evolution," *Electrical Engineering*, vol. 104, p. 2589–2602, 2022.
- [32] F. Wu, P. Zheng, L. Cheng, and C. Zhou, "Analysis and experimental evaluation of harmonic leakage inductance for polyphase pm machines having close slot and pole combinations," *IEEE Transactions on Magnetics*, vol. 51, no. 11, pp. 1–4, 2015.
- [33] K. Marouani, L. Baghli, D. Hadiouche, A. Kheloui, and A. Rezzoug, "A new pwm strategy based on a 24-sector vector space decomposition for a six-phase vsi-fed dual stator induction motor," *IEEE Transactions on Industrial Electronics*, vol. 55, no. 5, pp. 1910–1920, 2008.
- [34] S. Yang, P. Zheng, Y. Sui, C. Tong, and M. Wang, "Open-circuit fault-tolerant control for pentagon winding connected five-phase current-source inverter based pmsm drives," *IEEE Transactions on Industrial Electronics*, vol. 71, no. 3, pp. 2277–2288, 2024.
- [35] A. Sierra-Gonzalez, P. Pescetto, F. Alvarez-Gonzalez, B. Heriz, E. Trancho, H. Lacher, E. Ibarra, and G. Pellegrino, "Full-speed range control of a symmetrical six-phase automotive ipmsm drive with a cascaded dc-link configuration," *IEEE Transactions on Industry Applications*, vol. 59, no. 3, pp. 3413–3424, 2023.
- [36] G. Singh, "Multi-phase induction machine drive research—a survey," *Electric Power Systems Research*, vol. 61, no. 2, pp. 139–147, 2022.
- [37] Y. Chen, C. Liu, S. Liu, and Y. Liu, "Predictive control scheme with adaptive overmodulation for a five-leg vsi driving dual pmsms," *IEEE Transactions on Industrial Electronics*, vol. 71, no. 1, pp. 71–81, 2024.
- [38] J. Pyrhonen, T. Jokinen, and V. Hrabovcová, *Design of rotating electrical machines*. New Delhi, India: John Wiley & Sons, 2009.
- [39] G. Müller and B. Ponick, *Theorie elektrischer Maschinen*, 6th ed., ser. Elektrische Maschinen. Wiley-VCH Verlag GmbH & Co KGaA, 2009.
- [40] A. O. D. Tommaso, F. Genduso, and R. Miceli, "A new software tool for design, optimization, and complete analysis of rotating electrical machines windings," *IEEE Transactions on Magnetics*, vol. 51, no. 4, pp. 1–10, 2015.
- [41] M. Caruso, A. O. D. Tommaso, R. Miceli, and R. Rizzo, "The use of slightly asymmetrical windings for rotating electrical machines," *International Transactions on Electrical Energy Systems*, 2018.



a researcher at the Department of Engineering, University of Palermo, Italy.

Nicola Campagna received the M.S. and Ph.D. degrees in electrical engineering from the University of Palermo, Italy, in 2019 and 2023, respectively. In 2022, he joined the Electrotechnical Engineering Department of the Nova University of Lisboa working on the design of Wireless Power Transfer Systems for Automotive. In 2019 He joined the Sustainable Development and Energy Saving Laboratory, University of Palermo, Italy, focusing his research activities on the design of power electronics converter and energy storage systems. He is actually



simulation and experimental development of electrical machines and drives for industrial and sustainable energy applications. He is currently a reasecher at the Department of Engineering, University of Palermo, Italy.

Massimo Caruso received the M.S. and Ph.D. degrees in electrical engineering from the University of Palermo, Italy, in 2008 and 2012, respectively. In 2011, he joined the MEMS Sensors and Actuators Laboratory Group, University of Maryland, College Park, MD, USA, collaborating for the development of electric micromotors and drives for in vivo bacteria biofilm detection and treatment. In 2014, he joined the Sustainable Development and Energy Saving Laboratory, University of Palermo, Italy, focusing his research activities on the design,



design of electrical rotating machines.

Antonino Oscar Di Tommaso received the Master's and Ph.D. degrees in electrical engineering from the University of Palermo, Italy, in 1999 and 2004, respectively. He was a Post Ph.D. Fellow of Electrical Machines and Drives with the Department of Electrical Engineering, University of Palermo, from 2004 to 2006. He is currently an Associate Professor of Electrical Machines with the Department of Engineering, University of Palermo. His research interests include electrical machines, drives, diagnostics on power converters, and diagnostics and



Reviewer for the IEEE Transactions on Industrial Electronics and the IEEE Transactions on Industry Applications.

Rosario Miceli received the B.S. degree in electrical engineering and the Ph.D. degree from the University of Palermo, Palermo, Italy, in 1982 and 1987, respectively. He is a Full Professor of electrical machines with the Polytechnic School, University of Palermo. He is a Personnel in Charge of the Sustainable Development and Energy Savings Laboratory of the Palermo Athenaeum. His main research interests include mathematical models of electrical machines, drive system control, and diagnostics, renewable energies, and energy management. Dr. Miceli is a